ChemComm

COMMUNICATION

View Article Online
View Journal

Cite this: DOI: 10.1039/d3cc02336b

Received 13th May 2023,
Accepted 5th July 2023

DOI: 10.1039/d3cc02336b

rsc.li/chemcomm

Bis(naphthobipyrrolyl)methene-derived hexapyrrolic BODIPY as a single-molecule helicate with near-infrared emission†‡

Sipra Sucharita Sahoo and Pradeepta K. Panda *

Helically twisted bis(naphthobipyrrolyl)methene-derived open-chain hexapyrroles have been synthesized as HCl salts and the corresponding BODIPY. Their solid-state structures elucidated by single-crystal X-ray diffraction analysis clearly showed the presence of intramolecular hydrogen bonds, which were concluded to play a pivotal role in stabilizing the twisted conformation. Both molecules were observed to be NIR active, with the BODIPY moiety emission extending beyond 800 nm.

Molecular geometry plays a significant role in governing many of the properties of molecules from optical behaviour to coordination ability. On the other hand, geometry is controlled by intermolecular and intramolecular interactions such as steric crowding, non-covalent interactions such as van der Waals forces, hydrogen bonding, *etc.* The importance of helical geometry in biological systems became evident with the elucidation of the double helix structure of DNA.[1] Helicity represents a class of chirality known as axial chirality due to the presence of a stereogenic axis instead of a stereocentre.[2] Formation of helicity in rigid polyaromatic hydrocarbons (PAHs) is governed by steric hindrance between the terminal groups with a counterpoise of torsional strain due to twisting in the backbone.[3] However, intermolecular or intramolecular interactions such as hydrogen bonding play a crucial role in stabilizing the geometry in flexible molecules.[4]

Most helicenes, being polyaromatic fused systems, are endowed with interesting optical properties owing to extended π-conjugation. This feature makes them potential candidates for chiroptical devices and *in vivo* bioimaging probes.[5,6] However, they exhibit absorption and emission in the UV-Vis region with few of the PAHs extending their optical activities to the near-infrared (NIR) region.[7] The NIR-active PAHs consisting of large π-extended systems, such as hexa-peri-hexabenzocoronene-based [7]helicene ($C_{111}H_{30}(CO)_2(^tBu)_8$) with λ_{em} at 610 nm (ϕ_f = 0.09) or [9]helicene ($C_{198}H_{72}(^tBu)_6(^nhex)_{12}$) with a λ_{em} at 870 nm (ϕ_f = 0.04), need bulkier substituents to make them soluble, making them synthetically challenging.[8,9] Introducing electron-rich heterocyclic systems such as pyrrole, furan or thiophene into helicenes to form heterohelicenes can alter the optoelectronic properties of the helicenes due to the heterocyclic systems having vacant orbitals or lone pairs that can participate in conjugation.[10] These heterocyclic systems can reduce the HOMO–LUMO energy gap. Open-chain oligopyrroles and macrocycles are widely investigated scaffolds which can adopt helical conformations owing to their ability to have multiple non-covalent interactions such as hydrogen bonding.[4,10a] Also, their metal-coordinating and anion-binding abilities can induce formation of helical conformations in oligomers.[11] And they exhibit intense absorption and emission in the visible and NIR regions. Research is continuing apace to find new NIR-active helical dyes.

BODIPYs have been one of the frontline fluorophores in material science due to their interesting properties such as sharp and intense absorption and emission with good molar absorption coefficients and fluorescence quantum yields.[12] They also exhibit excellent photostability. Induction of helicity in BODIPY is a prospective approach for investigating BODIPY-based chiroptical devices. A literature search revealed a few reports about BODIPYs having been attached to helicenes to endow the helicenes with the optical properties of the BODIPYs, with one such example being compound **I** (Fig. 1).[13] However, the BODIPY skeleton endowed with helical conformation has hardly been observed (Compounds **II** and **III** in Fig. 1).[14]

Previously we reported about bis(naphthobipyrrolyl)methene-derived BODIPY **VIII**, which displays a planar structure and exhibits NIR absorption and emission at wavelengths of 727 and 744 nm, respectively.[15] However, we recently found—upon functionalizing the BODIPY at its free α,α′-positions in order to tune its optical properties and photodegradation and the

School of Chemistry University of Hyderabad, Hyderabad-500046, India.
E-mail: pradeepta.panda@uohyd.ac.in, pkpsc@uohyd.ernet.in

† Dedicated to Professor Jonathan L. Sessler on his 65th birthday.

‡ Electronic supplementary information (ESI) available. CCDC 2262189 and 2262190. For ESI and crystallographic data in CIF or other electronic format see DOI: https://doi.org/10.1039/d3cc02336b

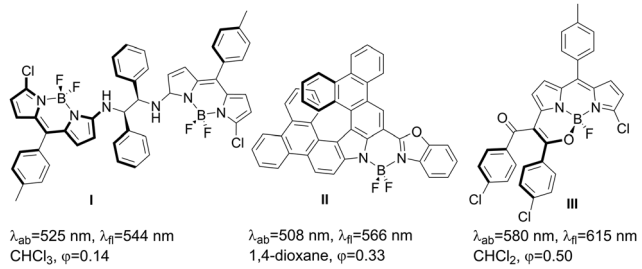

Fig. 1 Examples of helical BODIPYs with their optical properties.

substituents also induced formation of various degrees of non-planarity in the resultant derivatives.[16] Herein, we report a synthesis of a bis-(naphthobipyrrolyl)methene-derived hexapyrrolic helical BODIPY, which was found to exhibit NIR absorption and emission. The structure was stabilized by intramolecular hydrogen bonding between terminal ester groups and the uncomplexed pyrrolic units. Furthermore, insertion of boron was found to induce formation of a greater twist in the molecular skeleton, hence yielding a helical conformation.

The present work was initiated through serendipity. Our group along with others have been engaged in investigating the unique effects of *β,β′*-bipyrrole fusion on the photophysical features and coordination chemistry of porphyrinoids, including porphycene (an isomer of porphyrin) having no parallel chemistry in their non-fused analogues.[17] In this regard, we were interested in determining the effect of *β,β′*-bipyrrole fusion on the chemistry of corrphycene, another closely related isomer of porphyrin.[18] However, synthesis of the precursor tetrapyrrole having the naphthobipyrrole moiety from the corresponding dialdehyde eluded us (Scheme S1, ESI‡). Therefore, we redesigned our approach to synthesize the desired tetrapyrrole derivative by carrying out an acid-catalysed condensation of naphthobipyrrole **IV** with the acetoxypyrrole **V**. This condensation resulted in the formation of the desired product **VI**, along with the dipyrromethane **VII** and another unknown product (Scheme 1). Although we could unequivocally confirm the formation of **VI** through single-crystal X-ray diffraction analysis (Fig. S16, ESI‡), the similar polarities and melting points of **VI** and **VII** made their large-scale separation very difficult. On the other hand, successful elucidation of the crystal structure of the unknown product revealed formation of an unusual hexapyrrolic diester **1** as its hydrochloride salt, albeit in only 6% yield. Strikingly, this molecule displayed a helical structure (Fig. 2a). Subsequently, we changed the acid catalyst to $POCl_3$, which resulted in the formation of **1** in enhanced yield (26%). Attempts to further oxidize **1** failed, presumably due to involvement of pyrrolic NHs in intramolecular hydrogen bonding, which would be disrupted upon oxidation. Treating **1** with triethyl amine and subsequently with $BF_3{\cdot}OEt_2$ resulted in the formation of mono-BF_2 complex **2** with 60% yield (Scheme 1). As an alternative, we also tried carrying out a condensation of the acetoxy pyrrole ester **V** with the previously reported BODIPY **VIII**. Although we successfully used this procedure to synthesize the mono-BF_2 complex **2**, overall similar yields from naphthobipyrrole were found for both routes. Therefore, the strategy *via* hexapyrrole hydrochloride as a building block was found to be more suitable owing to the fewer steps involved. Both **1** and **2** were fully characterized by carrying out ^1H, ^{13}C, and ^{19}F spectroscopy investigations, HRMS analyses, and UV-Vis-NIR spectroscopy and their structures in the solid state were determined from single-crystal X-ray diffraction analyses.

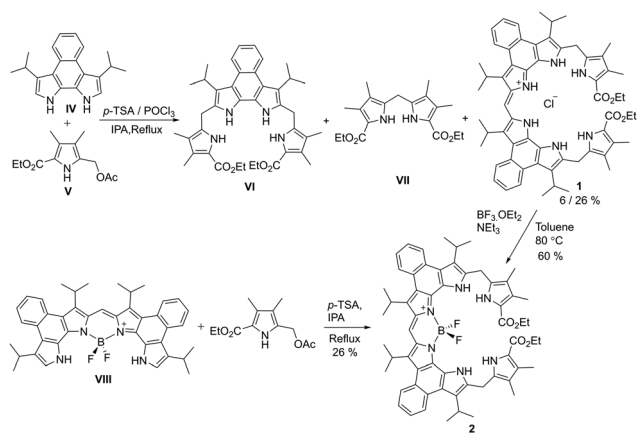

Scheme 1 Synthesis of bis(naphthobipyrrolyl)methene-derived BODIPY **2**.

The acquired ^1H NMR spectrum of **1** exhibited signals for 3 sets of deshielded NH protons, at 12.60, 11.72 and 11.29 ppm. Along with 4 sets of naphthalene peaks, one singlet (1 H) appeared at 7.95 ppm (Fig. S1, ESI‡). Another singlet (4 protons) appeared at 4.43 ppm along with signals for i-Pr CH and ester CH_2 protons. This result indicated that only one *meso*-carbon was oxidized while the other two remained unoxidized. The complexation with BF_2 was confirmed with the absence of signals for two NHs in the ^1H NMR spectrum (Fig. S3, ESI‡). The signals for the other four NHs were present but two of them were shifted upfield owing to a loss of hydrogen bonding with Cl^- ion.

A single-crystal X-ray diffraction (SCXRD) analysis of a diffraction-grade crystal (obtained from slow evaporation of chloroform) revealed the helical conformation of **1**. Inspection of the structure showed two naphthobipyrroles tethered together by a *meso*-methine bridge and two dimethyl pyrrole derivatives attached to both ends of the bisnaphthobipyrrolylmethene with two *meso*-type methylene bridges (Fig. 2). Observed was a twist *via* the *meso*-methine bridge and distorted naphthobipyrroles, features resulting in the structure adopting a helical conformation. The conformation was apparently stabilized by six intramolecular hydrogen bonds, four between naphthobipyrrolic NHs and Cl^- ion, and other two between ester carbonyl oxygens and pyrrolic NHs (Fig. 2a and b). A dihedral angle of 20.73° between two naphthobipyrrole units was measured (Fig. 2e). The chloride ion was observed to be positioned slightly closer to the outer two nitrogens of bis(naphthobipyrrolyl)methene (3.11(4) Å) than the inner two nitrogens (3.18(3) Å). Inspection of the structure showed the outer two pyrrole esters facing each other with the ester carbonyl oxygen positioned directly above the opposite pyrrole

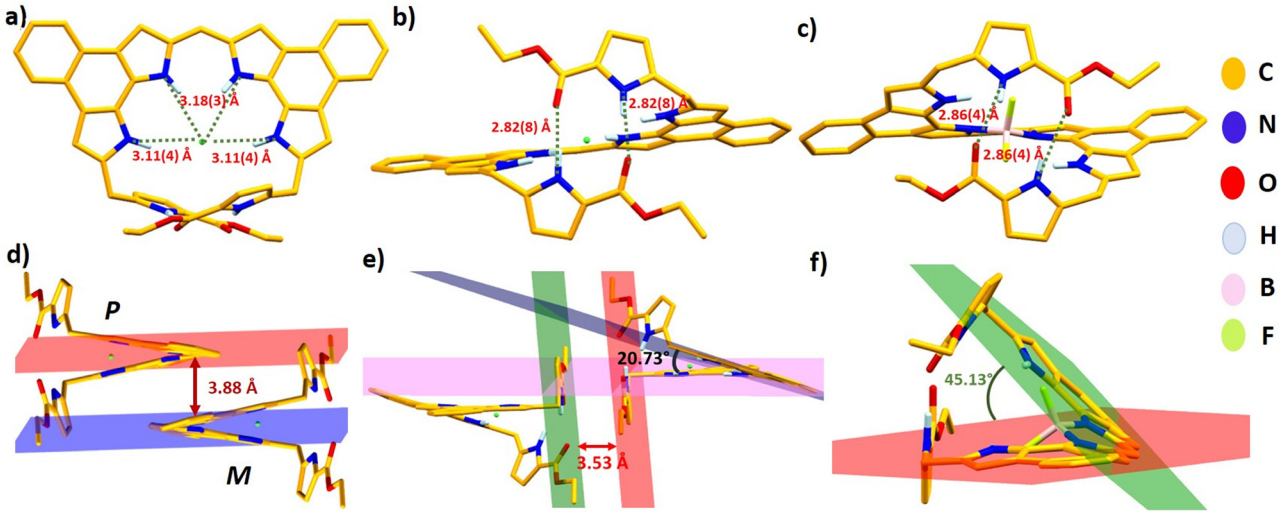

Fig. 2 Crystal structures of **1** and **2** showing different views and π–π stacking interactions. Peripheral substituents and hydrogen atoms were removed for clarity.

NH with an O-N distance of 2.82(8) Å (Fig. 2b). Inspection of the packing diagram demonstrated the *P* and *M* enantiomers alternating in a 1 : 1 ratio, making the system racemic (Fig. S14, ESI‡). Two types of π–π stacking interactions in the crystal packing were identified: one between two bis(naphthobipyrrolyl)methene planes of the alternating enantiomers along the *b*-axis with an interplanar distance of 3.88 Å (Fig. 2d); the other being π–π interactions between the outer pyrroles of the two racemates along the *c*-axis with an interplanar distance of 3.53 Å (Fig. 2e). The acquired SCXRD structure of **2** was elucidated from a diffraction-grade crystal obtained by carrying out a slow diffusion of hexane into a chloroform solution of the compound. The structural analysis revealed the naphthobipyrrole units to be much more twisted than **1** and specifically to be related by a dihedral angle of 45.13° (Fig. 2f). The intramolecular NH···O hydrogen bond strengths for **2** were indicated to be slightly reduced, with a distance of 2.86(4) Å measured between the pyrrolic nitrogen and carbonyl oxygen of the ester (Fig. 2c). Inspection of the packing diagram showed the presence of both *P* and *M* enantiomers (Fig. S15, ESI‡). On the other hand, the intermolecular interactions were slightly enhanced with outer pyrroles of alternatively placed enantiomers showing π–π interactions with an interplanar distance of 3.45 Å (Fig. S15, ESI‡).

Compound **1** exhibited intense absorption at 758 nm accompanied with a high-energy band at 693 nm and near-UV band at 468 nm. This compound also showed solvent-dependent absorption (Fig. 3b and Fig. S8, ESI‡). For example, with increasing polarity of solvent, it displayed hypsochromic shifting along with a decreasing molar absorption coefficient. Furthermore, in highly polar solvent such as methanol or DMSO, it yielded a spectrum not showing the structured sharp and intense peak, but instead a blue-shifted broad peak with reduced intensity as shown in Fig. 3b. This result may be attributed to a solvent-induced deprotonation. To lend further credence to this deprotonation, we recorded an absorption spectrum of **1** in the presence of excess triethyl amine to induce

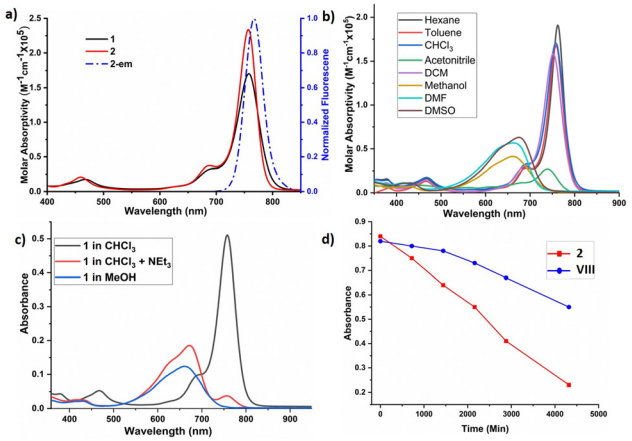

Fig. 3 (a) Absorption and emission spectra of **1** and **2** in $CHCl_3$; (b) absorption spectra of **1** in various solvents (3 μM); (c) deprotonation of **1**; (d) photodegradation of **2** in toluene (3 μM).

deprotonation, and a similar feature was observed (Fig. 3c). Compound **2** exhibited a very similar absorption profile, but the peak at 757 nm was relatively sharp with a reduced full width at half maximum (FWHM), a typical characteristic of BF_2-complexation (Tables S1 and S2, ESI‡). Unlike **1**, compound **2** did not show any considerable solvatochromism in the ground-state absorption spectra. While **1** was found to be non-emissive, BODIPY **2** was quite emissive (λ_{emi} = 767 nm; Δ_ϕ: 0.14–0.27 and Table S2, ESI‡). It exhibited a fluorescence lifetime of 4.01 ns in chloroform. The emission spectra of **2** exhibited a positive solvatochromism resulting in a higher Stokes shift in polar solvents such as methanol and DMSO, indicating intramolecular charge transfer in the excited state (Fig. S11, ESI‡). Note that the structures of **1** and **2** showed no extension of π-conjugation beyond that displayed by the α,α′-free naptho-BODIPY **VIII**, and thus the observed bathochromic shift in both absorption and emission may be attributed to the structural

distortion from planarity to helicity. Photostability of the BODIPY derivative was examined by constantly irradiating its air-saturated solution with 365-nm-wavelength light from a lamp (8 W) for 72 h (Fig. 3d). To examine the effect of structural modification on photostability, we compared **2** with **VIII** under similar conditions. Compound **2** showed a higher rate of photodegradation (1% decomposition per 1.2 h) than did **VIII** (1% per 3 h), which may be attributed to the presence of two unoxidized *meso*-type bridging methylene moieties in **2**.

Cyclic voltammograms of both **1** and **2** exhibited a quasi-reversible 1st oxidation (E_{ox}^{1}) and reduction (E_{red}^{1}) potential (Fig. S13, ESI‡). Boron complexation of **1** facilitated the oxidation in **2** while reduction became difficult. However, both compounds exhibited multiple redox potentials, which can be attributed to the presence of redox-active functional groups and *meso*-type methylene units.

The structure of the ground state of **2** in the gas phase was optimized by performing DFT calculations with the B3LYP method and 6-31G(d,p) basis set. The gas-phase structure was found to exhibit a reduced twist in its naphthobipyrrole units with a dihedral angle of 32.50° (Fig. S17, ESI‡). The distances between the oppositely faced pyrrolic N atoms and ester carbonyl O atoms were measured to be 2.87 and 2.88 Å, in good agreement with the structure of the solid state. The corresponding frontier orbital diagrams showed both the HOMO and LUMO coefficients were concentrated on the bis(naphthobipyrrolyl)methene unit. The calculations indicated a smaller HOMO–LUMO gap for **2** (2.0 eV) than for planar **VIII** (2.05 eV) (Fig. S18, ESI‡), consistent with the bathochromic shift of **2** in an acquired experimental absorption spectrum. A TD-DFT calculation showed the lowest energy transition to be purely from HOMO to LUMO (Table S4, ESI‡).

In summary, we have synthesized an NIR-active bis(naphthobipyrrolyl)methene-derived open-chain hexapyrrole and an NIR-emissive BODIPY analogue (ϕ_f = 0.27), with both of them shown to adopt stable helical conformations. Solid-state structural analysis revealed a role of intramolecular hydrogen bonding in stabilizing the helical conformation. The synthesised NIR-active BODIPY has potential applications in chiral resolution and in chiral photoluminescent (CPL) devices.

This work was supported by Institute of Eminence (IoE), University of Hyderabad (Project No. RC1-20-001) and SERB, India (project no. EMR/2017/003109). S. S. S. thanks UGC, India and IoE for financial support. The authors thank K. S. Srivishnu (IICT, Hyderabad) for his help in fluorescence lifetime measurements. The authors are grateful for access to the computational facility of CMSD, University of Hyderabad. The authors also thank Mr Mahesh S. Rathod and Dr Babu Vargese (SAIF, IIT Madras) for their help in solving and carrying out refinement of crystal structures.

Conflicts of interest

There are no conflicts to declare.

References

1 J. D. Watson and F. C. H. Crick, *Nature*, 1953, **171**, 737.
2 Y. Shen and C.-F. Chen, *Chem. Rev.*, 2012, **112**, 1463.
3 M. Rickhaus, M. Mayor and M. Juŕíček, *Chem. Soc. Rev.*, 2016, **45**, 1542.
4 G. D. Pantoş, M. S. Rodríguez-Morgade, T. Torres, V. M. Lynch and J. L. Sessler, *Chem. Commun.*, 2006, 2132.
5 (*a*) Y. Yang, R. C. Da. Costa, M. J. Fuchter and A. J. Campbell, *Nat. Photonics*, 2013, **7**, 634; (*b*) Y. Liu, Z. Ma, Z. Wang and W. Jiang, *J. Am. Chem. Soc.*, 2022, **144**, 11397.
6 Y.-F. Wu, S.-W. Ying, L.-Y. Su, J.-J. Du, L. Zhang, B.-W. Chen, H.-R. Tian, H. Xu, M.-L. Zhang, X. Yan, Q. Zhang, S.-Y. Xie and L.-S. Zheng, *J. Am. Chem. Soc.*, 2022, **144**, 10736.
7 (*a*) Y. Nakakuki, T. Hirose and K. Matsuda, *J. Am. Chem. Soc.*, 2018, **140**, 15461; (*b*) J. Tan, X. Xu, J. Liu, S. Vasylevskyi, Z. Lin, R. Kabe, Y. Zou, K. Müllen, A. Narita and Y. Hu, *Angew. Chem., Int. Ed.*, 2023, e202218494.
8 C. M. Cruz, S. Castro-Fernández, E. Maçôas, J. M. Cuerva and A. G. Campaña, *Angew. Chem., Int. Ed.*, 2018, **57**, 14782.
9 Y. Wang, Z. Yin, Y. Zhu, J. Gu, Y. Li and J. Wang, *Angew. Chem., Int. Ed.*, 2019, **58**, 587.
10 (*a*) K. Ueta, M. Umetani, A. Osuka, G. D. Pantoş and T. Tanaka, *Chem. Commun.*, 2021, **57**, 2617; (*b*) A. Bucinskas, D. Waghray, G. Bagdziunas, J. Thomas, J. V. Grazulevicius and W. Dehaen, *J. Org. Chem.*, 2015, **80**, 2521; (*c*) G. M. Upadhyay, H. R. Talele and A. V. Bedekar, *J. Org. Chem.*, 2016, **81**, 7751; (*d*) K. Dhbaibi, L. Favereau and J. Crassous, *Chem. Rev.*, 2019, **119**, 8846.
11 (*a*) Y. Haketa and H. Maeda, *Chem. – Eur. J.*, 2011, **17**, 1485; (*b*) Y. Haketa, Y. Bando, K. Takaishi, M. Uchiyama, A. Muranaka, M. Naito, H. Shibaguchi, T. Kawai and H. Maeda, *Angew. Chem., Int. Ed.*, 2012, **51**, 7967; (*c*) H. Maeda, T. Nishimura, R. Akuta, K. Takaishi, M. Uchiyamabd and A. Muranaka, *Chem. Sci.*, 2013, **4**, 1204; (*d*) C. Eerdun, S. Hisanaga and J.-I. Setsune, *Angew. Chem., Int. Ed.*, 2013, **52**, 929; (*e*) M. Saikawa, T. Nakamura, J. Uchida, M. Yamamura and T. Nabeshima, *Chem. Commun.*, 2016, **52**, 10727; (*f*) C. Eerdun, T. H. T. Nguyen, T. Okayama, S. Hisanaga and J.-I. Setsune, *Chem. – Eur. J.*, 2019, **25**, 5777.
12 (*a*) A. Loudet and K. Burgess, *Chem. Rev.*, 2007, **107**, 4891; (*b*) N. Boens, V. Leen and W. Dehaen, *Chem. Soc. Rev.*, 2012, **41**, 1130; (*c*) M. Poddar and R. Misra, *Coord. Chem. Rev.*, 2020, **421**, 213462.
13 (*a*) Z. Liu, Z. Jiang, C. He, Y. Chen and Z. Guo, *Dyes Pigm.*, 2020, **181**, 108593; (*b*) C. Maeda, K. Nagahata, T. Shirakawa and T. Ema, *Angew. Chem., Int. Ed.*, 2020, **59**, 7813.
14 (*a*) E. M. Sánchez-Carnerero, F. Moreno, B. L. Maroto, A. R. Agarrabeitia, J. Bañuelos, T. Arbeloa, I. López-Arbeloa, M. J. Ortiz and S. Moya, *Chem. Commun.*, 2013, **49**, 11641; (*b*) Z. Zhou, J. Zhou, L. Gai, A. Yuan and Z. Shen, *Chem. Commun.*, 2017, **53**, 6621; (*c*) Z. Wang, L. Huang, Y. Yan, A. M. El-Zohry, A. Toffoletti, J. Zhao, A. Barbon, B. Dick, O. F. Mohammed and G. Han, *Angew. Chem., Int. Ed.*, 2020, **59**, 16114; (*d*) L.-Y. Wang, Z.-F. Liu, K.-X. Teng, L.-Y. Niu and Q.-Z. Yang, *Chem. Commun.*, 2022, **58**, 3807.
15 T. Sarma, P. K. Panda and J.-I. Setsune, *Chem. Commun.*, 2013, **49**, 9806.
16 S. S. Sahoo, T. Sarma, K. S. Srivishnu and P. K. Panda, *Chem. – Eur. J.*, 2023, e202300942.
17 (*a*) T. Sarma, P. K. Panda, P. T. Anusha and S. V. Rao, *Org. Lett.*, 2011, **13**, 188; (*b*) M. Ishida, S.-J. Kim, C. Preihs, K. Ohkubo, J. M. Lim, B. S. Lee, J. S. Park, V. M. Lynch, V. V. Roznyatovskiy, T. Sarma, P. K. Panda, C.-H. Lee, S. Fukuzumi, D. Kim and J. L. Sessler, *Nat. Chem.*, 2013, **5**, 15; (*c*) T. Sarma, P. T. Anusha, A. Pabbathi, S. V. Rao and P. K. Panda, *Chem. – Eur. J.*, 2014, **20**, 15561; (*d*) T. Sarma, B. S. Kumar and P. K. Panda, *Angew. Chem., Int. Ed.*, 2015, **54**, 14835; (*e*) T. Kim, Z. Duan, S. Talukdar, C. Lei, D. Kim, J. L. Sessler and T. Sarma, *Angew. Chem., Int. Ed.*, 2020, **59**, 13063; (*f*) S. Sahoo and P. K. Panda, *Inorg. Chem.*, 2022, **61**, 2707.
18 (*a*) J. L. Sessler, E. A. Brucker, S. J. Weghorn, M. Kisters, M. Schiifer, J. Lex and E. Vogel, *Angew. Chem., Int. Ed. Engl.*, 1994, **33**, 2308; (*b*) R. Nozawa and H. Shinokubo, *Org. Lett.*, 2017, **19**, 4928.

